A new ultrafast technique for measuring the terahertz dynamics of chiral molecules: The theory of optical heterodyne-detected Raman-induced Kerr optical activity

Klaas Wynne[a)]
Department of Physics, University of Strathclyde, Glasgow G4 0NG, Scotland, United Kingdom

(Received 9 March 2005; accepted 27 April 2005; published online 27 June 2005)

Optical heterodyne-detected Raman-induced Kerr optical activity (OHD-RIKOA) is a nonresonant ultrafast chiroptical technique for measuring the terahertz-frequency Raman spectrum of chirally active modes in liquids, solutions, and glasses of chiral molecules. OHD-RIKOA has the potential to provide much more information on the structure of molecules and the symmetries of librational and vibrational modes than the well-known nonchirally sensitive technique optical heterodyne-detected Raman-induced Kerr-effect spectroscopy (OHD-RIKES). The theory of OHD-RIKOA is presented and possible practical ways of performing the experiments are analyzed. © *2005 American Institute of Physics*. [DOI: 10.1063/1.1937390]

I. INTRODUCTION

Low-frequency librational and vibrational modes in the condensed phase with a frequency of about a terahertz are important in understanding the fluctuations that drive and stabilize reactions. Terahertz-frequency fluctuations in liquids control the rates of chemical reactions and similar motions in proteins control protein-folding rates and the rates of enzymatic reactions. Such low-frequency modes have been studied with various forms of infrared absorption, Raman scattering, and other spectroscopies for decades. One especially sensitive technique is based on the ultrafast Kerr effect and is often referred to as optical heterodyne-detected Raman-induced Kerr-effect spectroscopy (OHD-RIKES).[1] OHD-RIKES has been applied to a great variety of condensed-phase systems such as polar[2–4] and nonpolar liquids,[5,6] liquid crystals,[7,8] liquid mixtures,[9] solutions,[10] protein solutions,[11–13] and other inhomogeneous media.[14,15] Typical OHD-RIKES spectra cover the approximate range of 0.3 to $>500\ \mathrm{cm}^{-1}$ corresponding to time scales of about 50 fs to 100 ps. At very low frequencies ($<\sim 10\ \mathrm{cm}^{-1}$), the signal is mostly due to diffusive reorientational motions of molecules or molecular side groups. At relatively high frequencies ($>\sim 200\ \mathrm{cm}^{-1}$), intramolecular vibrational modes and hydrogen-bond motions are observed. The intermediate region is in some sense of most interest and represents underdamped or critically damped librational motions of individual molecules or groups of molecules (collective motions).

Figure 1 shows a typical example of an OHD-RIKES spectrum of benzonitrile emphasizing the intermediate frequency range. Such a spectrum is typically fitted with a number of analytical line shapes. Many groups have used combinations of Lorentzian, Ohmic, and Gaussian lineshapes[1] to fit such spectra, whereas others have used distributions of harmonic oscillators as in Fig. 1.[4,16] It is quite clear, however, that, despite the impressive signal-to-noise ratio achievable in the OHD-RIKES experiments, such fits are somewhat arbitrary as the results depend on the choice of fit functions.

Different spectroscopies have been applied in combination with OHD-RIKES in the hope to extract more information about the modes in the intermediate frequency region. For example, OHD-RIKES and low-frequency spontaneous Raman-scattering spectra have been compared with far-infrared-absorption spectra.[4,6] OHD-RIKES experiments have also been compared with inelastic neutron-scattering spectra.[13] It has been suggested[4] that the infrared and Raman spectra of liquids can be described by a single set of oscillators with different relative strengths in the two types of spectroscopy. However, this may not be applicable in nonpolar liquids.[6]

In principle, off-resonant six- and eight-wave mixing experiments[17] can be used to access information that is unavailable from the OHD-RIKES type experiments. These higher-order techniques have been applied to liquids[18,19] but the interpretation of the results is hampered by the presence of contamination from cascaded lower-order processes.[19,20] In a quite different approach, a solvated dye molecule is resonantly excited and the subsequent solvent response

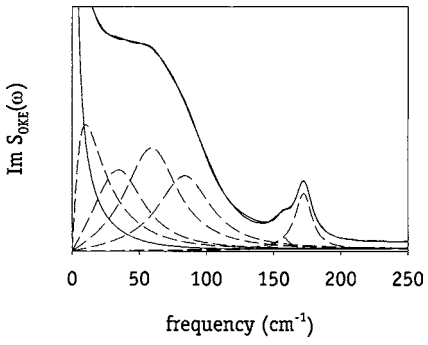

FIG. 1. Optical heterodyne-detected Raman-induced Kerr-effect spectrum (OHD-RIKES) of benzonitrile and analysis in terms of six Brownian oscillators (see Ref. 4).

[a)]Electronic mail: klaas.wynne@phys.strath.ac.uk

probed through an off-resonant Kerr process.[21] Such experiments provide novel information on the coupling between solutes and the surrounding bath but do not necessarily provide any more information on the nature and distribution of the intermediate frequency solvent modes.

It has been shown[22] to be possible to modify the OHD-RIKES technique by spatially masking the probe beam, allowing the direct measurement of individual tensor components. Using this technique, one can separately measure the anisotropic and isotropic invariants of the molecular polarizability tensor. Unfortunately, for the intermediate frequency collective modes in liquids, the anisotropic invariant is significantly larger than the isotropic invariant[8,22] and the isotropic spectrum is very similar in shape to the anisotropic spectrum. Significant differences between the isotropic and anisotropic spectra can only be seen at high frequencies in hydrogen-bonding liquids and proteins.[12,22]

Thus, the problem remains that there is no reliable method to separate the various modes supposedly present in the intermediate frequency Raman spectrum of liquids and proteins. A similar problem exists for Raman scattering off high-frequency modes in some cases. For example, Raman scattering has been used to study the amide bands of proteins but congestion and broadening make it difficult to extract structural information. In 1969, it was predicted that the light-scattered off chiral molecules contain a small degree of circular polarization.[23] Further improvement of this idea led to the development of Raman optical activity (ROA),[24] which is now a mature technique used in commercial instruments.[25–27] ROA and the related infrared-absorption technique of vibrational circular dichroism[28] (VCD) produce spectra with bands for those modes that change with the chirality of the molecule. ROA and VCD both require the sample to be optically active (rather than a racemic mixture). The strength and sign of the spectral bands are directly related to the structure and handedness of the molecule and can be used in conjunction with *ab initio* computations to determine the absolute three-dimensional configuration of molecules.

It is well known that spontaneous Raman scattering and OHD-RIKES are related and contain essentially the same information.[29] Both spontaneous Raman scattering and OHD-RIKES are four-wave mixing processes where the former involves vacuum fluctuations and the latter externally supplied pump- and probe-laser beams. Therefore, it is clear that an optical-activity version of OHD-RIKES ought to exist. Coherent versions of ROA such as coherent anti-Stokes Raman scattering (CARS) (Ref. 30) and other chiral four-wave mixing phenomena[31,32] have been considered before but not any nonlinear process related to OHD-RIKES. The content of the ROA spectrum depends on the scattering angle[33] and the optimum result is obtained in a backscattering geometry. However, OHD-RIKES is an ultrafast experiment relying on femtosecond time resolution and could therefore not easily be performed at any other angle between pump and probe beams than about zero degrees. We have derived a theory for a ROA analog of OHD-RIKES, named optical heterodyne-detected Raman-induced Kerr optical activity (OHD-RIKOA) and will show that an optical-activity signal can be obtained in the forward direction under the right polarization conditions. At the end of this paper, we will show how an OHD-RIKOA signal could be measured in practice and how the much stronger (on the order of a factor of 1000 or more) OHD-RIKES signal can be suppressed.

II. THEORY

The experiment described here is a variation of optical heterodyne-detected Raman-induced Kerr-effect spectroscopy (OHD-RIKES) in which two beams of ultrashort laser pulses interact with an isotropic (typically liquid) and nonabsorbing (at the laser wavelength) sample. The pump beam propagating along the wave vector $\mathbf{k}^{\text{pump}}$ excites the sample perturbing the refractive index. The probe beam with wave vector $\mathbf{k}^{\text{probe}}$ is used to measure the decay of the refractive-index perturbation as a function of the delay between the pump- and probe-laser pulses. As in OHD-RIKES, the signal is proportional to the third-order susceptibility. However, unlike normal OHD-RIKES, here we will consider a more general interaction with not only the electric-dipole moment but also the magnetic-dipole moment and the electric-quadrupole moment. The interaction Hamiltonian is given by[27,29,32]

$$H = -\mu_i E_i(\mathbf{r},t) - m_i B_i(\mathbf{r},t) - \frac{1}{3} Q_{ij} \nabla_j E_i(\mathbf{r},t), \tag{1}$$

where $\mathbf{m}$ is the magnetic-dipole-moment vector and $\hat{Q}$ the quadrupole tensor.[27] Subscripts will be used throughout to identify tensor elements and Einstein summation convention is implied. The magnetic-dipole and electric-quadrupole interaction terms can be estimated[34] to be about three orders of magnitude smaller than the electric-dipole-moment interaction term. Therefore, in a chiroptical four-wave mixing experiment such as OHD-RIKOA only one interaction with either the magnetic-dipole or the electric-quadrupole moment has to be taken into consideration, the other three interactions being through the electric-dipole moment. Processes involving more than one interaction with the magnetic-dipole or the electric-quadrupole moment will be too small to be relevant.

For real wave functions, the electric-dipole-moment matrix element is real, i.e.,

$$\boldsymbol{\mu}^{eg} \equiv \langle e|\boldsymbol{\mu}|g\rangle = \boldsymbol{\mu}^{ge}, \tag{2}$$

whereas the magnetic-dipole-moment matrix element is purely imaginary:[32]

$$\mathbf{m}^{eg} = -\mathbf{m}^{ge} = i\mathbf{M}, \tag{3}$$

where $\mathbf{M}$ is real. The quadrupole tensor is real ($Q^{eg}=Q^{ge}$), symmetric, and traceless, i.e.,[27]

$$Q_{ij} = Q_{ji},\ Q_{ii} = Q_{xx} + Q_{yy} + Q_{zz} = 0. \tag{4}$$

In the derivation below, use will be made of the slowly varying envelope approximation[35] and the electric and magnetic fields will be written as

$$\mathbf{E}(\mathbf{r},t) = \frac{1}{2}E^0 f(t)\mathbf{e}\exp(-i\omega_0 t + i\mathbf{k}\cdot\mathbf{r}) + \text{c.c.},$$
$$\mathbf{B}(\mathbf{r},t) = \frac{1}{2}B^0 f(t)\mathbf{b}\exp(-i\omega_0 t + i\mathbf{k}\cdot\mathbf{r}) + \text{c.c.}, \tag{5}$$

where E^0 and B^0 are the field amplitudes and $f(t)$ is the pulse envelope. It will be assumed that all the laser fields involved are plane waves and the field vectors are related by $\mathbf{b}\equiv\boldsymbol{\kappa}\times\mathbf{e}$ where $\mathbf{e}$, $\mathbf{b}$, and $\boldsymbol{\kappa}\equiv\mathbf{k}/|\mathbf{k}|$ are all unit-length vectors. For plane waves, one also has the simple relationship $B^0=E^0/c$. Circularly polarized fields can be written in complex notation.[32,36] If $\mathbf{e}^{(1)}$ and $\mathbf{e}^{(2)}$ are two real and orthogonal vectors that are both orthogonal to $\boldsymbol{\kappa}$, then left and right circularly polarized electric-field waves have polarization vectors $\mathbf{e}^{(L)}=1/\sqrt{2}(\mathbf{e}^{(1)}+i\mathbf{e}^{(2)})$ and $\mathbf{e}^{(R)}=1/\sqrt{2}(\mathbf{e}^{(1)}-i\mathbf{e}^{(2)})$. The corresponding magnetic-field vectors are $\mathbf{b}^{(L)}=-i\mathbf{e}^{(L)}$ and $\mathbf{b}^{(R)}=i\mathbf{e}^{(R)}$.

For later use, it is helpful to write the interaction Hamiltonian in the following form:

$$\begin{aligned} H_I &= -\frac{1}{2}f(t)\exp(-i\omega_0 t + i\mathbf{k}\cdot\mathbf{r})\left[\mu_i e_i E^0 + m_i b_i B^0 + i\frac{1}{3}Q_{ij}k_j e_i E^0\right] - \frac{1}{2}f(t)\exp(+i\omega_0 t - i\mathbf{k}\cdot\mathbf{r}) \\ &\quad\times\left[\mu_i e_i^* E^0 + m_i b_i^* B^0 - i\frac{1}{3}Q_{ij}k_j e_i^* E^0\right] \\ &\equiv -\frac{1}{2}f(t)\exp(-i\omega_0 t + i\mathbf{k}\cdot\mathbf{r})(o^{(1/2/3)} + o^{(1/2/3)^*}). \end{aligned} \tag{6}$$

Here $o^{(1/2/3)}$ is the operator associated with the first, second, and third interactions with the field, which has matrix elements $o^{(1/2/3)nm}$. In the RIKOA four-wave mixing process, there is one interaction with the magnetic-dipole or the electric-quadrupole moment and three interactions with the electric-dipole moment. By using this form of the Hamiltonian, the choice of which operator to use with which field can be deferred to the last moment. As the magnetic-dipole or electric-quadrupole moment coupling can also be the fourth interaction, both the third-order polarization and the third-order magnetization have to be calculated. In order to keep the expressions simple, the expectation value of the operator $\hat{o}$ will be calculated (where $\hat{o}$ is either the electric-dipole, the magnetic-dipole, or the electric-quadrupole moment operator) resulting in a value for the third-order "*o*-ization" $\mathbf{O}(t)$.

In the OHD-RIKOA experiment as in a standard OHD-RIKES experiment, the field generated in third order is detected by heterodyning it with the external probe field. With the use of wave plates in the probe beam, one can heterodyne with in-phase or out-of-phase fields resulting in the detection of dichroic or refractive effects, respectively. The electromagnetic energy absorbed for an out-of-phase probe field is[37]

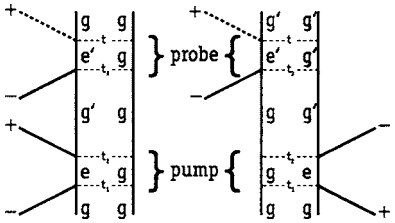

FIG. 2. The two most relevant Feynman paths for Raman-induced Kerr optical activity (RIKOA) and Raman-induced Kerr-effect spectroscopy (RIKES). In RIKES, all four field interactions are through the electric-dipole-moment operator. In RIKOA, one interaction is instead through the magnetic-dipole- or electric-quadrupole-moment operator. The first two interactions are assumed to be with the pump-laser field and the final two with the probe-laser field.

$$S_{\text{refrac}} = \text{Im}\int dt\left(\mathbf{E}\cdot\frac{\partial\mathbf{P}}{\partial t} + \mu_0\mathbf{H}\cdot\frac{\partial\mathbf{M}}{\partial t}\right) \tag{7}$$

and the real part for an in-phase probe field. In the slowly-varying envelope approximation, the derivative in the above equation can be replaced by a multiplication with $i\omega_0$. The above expression is only valid in the small signal limit.

A. Third-order *o*-ization in its most general form

The derivation of the RIKOA signal will be largely along the lines of previous theoretical treatments of OHD-RIKES.[38] The diagram in Fig. 2 shows the two principal Feynman interaction paths for RIKOA and these differ little from those describing RIKES. The pump laser interacts with the molecules in a second-order Raman interaction to produce a superposition state of two vibrational or librational states in the ground electronic state. The probe laser subsequently scatters off this superposition state in another Raman interaction to produce an *o*-ization (polarization or magnetization). It will be assumed that the laser is not resonant with any of the intermediate electronically excited states. Under that assumption, it is reasonable to ignore non rotating-wave[35] terms (those that have the first two or the last two interactions in Fig. 2 reversed). It is then also reasonable to ignore those terms where the pump and probe fields act out of order, since these will just lead to an instantaneous response. In OHD-RIKES experiments, this instantaneous response is referred to as the electronic response and is essentially ignored in the data analysis.

The double Feynman diagrams in Fig. 2 are not labeled with specific operators yet as the assignment of operators to interactions will be deferred as described earlier. From the form of the spatial part of the interaction operator in Eq. (6) and the diagrams in Fig. 2 it can be seen, however, that phase matching occurs when the wave vector of the *o*-ization coincides with the wave vector of the probe laser.

It is then straightforward to write down the third-order *o*-ization from the double Feynman diagrams in Fig. 2. As the fields are not resonant with the intermediate electronic states, it is possible to make the approximation

$$\lim_{\Delta\to\infty}\int_{-\infty}^{t_2} dt_1 E(t_1)e^{\pm i\Delta(t_2-t_1)} = \frac{E(t_2)}{\mp i\Delta}, \tag{8}$$

where $\Delta \equiv \Omega - \omega_0$ is the difference between the Bohr frequency Ω of the intermediate state and the laser carrier frequency. The third-order *o*-ization can then be written as

$$\mathbf{O}^{(3)} = \frac{N}{8}e^{-i\omega_0 t}e^{+i\mathbf{k}^{\text{probe}}\cdot\mathbf{r}} \times \int_0^\infty d\tau (f^{\text{pump}}(t-\tau))^2 f^{\text{probe}}(t)\frac{1}{(\hbar\Delta)^2} \times \begin{bmatrix} +\frac{i}{\hbar}\langle U_\nu(-\tau)\hat{o}^{ge}o^{(3)eg}U_\nu(\tau)o^{(2)*ge}o^{(1)eg}\rangle_Q \\ -\frac{i}{\hbar}\langle o^{(1)*ge}o^{(2)eg}U_\nu(-\tau)\hat{o}^{ge}o^{(3)eg}U_\nu(\tau)\rangle_Q \end{bmatrix}, \tag{9}$$

where N is the number density. In the above expression, $U_\nu(t)$ is the time-evolution operator of the vibrational/librational Hamiltonian[29] and

$$\langle\cdots\rangle_Q = \sum_g \rho_{gg}\langle g|\cdots|g\rangle \tag{10}$$

is a quantum-mechanical thermal average over the vibrational/librational state. The quantum correlation function in Eq. (9) is over vibrational operators, so the ordering is important. Strictly speaking, Eq. (9) is incorrect: It should include a sum over all possible intermediate electronically excited states. In the end, however, it will be found that this sum can be reintroduced without loss of generality.

B. Electric-dipole interaction: Birefringence

For purposes of comparison, the OHD-RIKES signal will be calculated first. In OHD-RIKES, all four interactions are with the electric-dipole-moment operator and the signal in Eq. (9) is the third-order polarization. Using Eq. (7) in the slowly varying amplitude approximation, it is found that the signal can be written as

$$S = \frac{N\omega_0}{16}(E^{0,\text{pump}})^2(E^{0,\text{probe}})^2\,\text{Re}\int_0^\infty d\tau G(\tau) \times T^{\text{RIKES}}\frac{i}{\hbar}\langle[q(\tau),q]_-\rangle_Q, \tag{11}$$

where

$$T^{\text{RIKES}} = \langle\alpha_{ij}\alpha_{kl}\rangle e_i e_j^* e_k e_l^* \tag{12}$$

and the angular brackets stand for an orientational average. In this expression,

$$\alpha_{ij} = \frac{d}{\hbar\Delta dq}\mu_i\mu_j = \alpha_{ji} \tag{13}$$

is the first derivative with respect to the vibrational coordinate of the polarizability tensor. Because the double Feynman diagrams in Fig. 2 do not include the counterrotating-wave paths, this definition of the polarizability tensor deviates somewhat from the standard definition that can be found elsewhere.[27] At this point one could reintroduce a sum over all the possible intermediate electronically excited states. In Eq. (11), the indices i and j refer to the pump-laser field, and k and l to the probe-laser field. In order to arrive at the compact form of Eq. (11), the indices i and j had to be exchanged, which is only possible when the laser is far off resonance and the equality on the right-hand side of Eq. (13) holds. The envelopes of the pump- and probe-laser pulses appear in

$$G(\tau) \equiv \int_{-\infty}^\infty dt (f^{\text{pump}}(t-\tau))^2 (f^{\text{probe}}(t))^2, \tag{14}$$

which is the laser-pulse cross-correlation function.

In deriving the expression for the OHD-RIKES signal in Eq. (11) from Eq. (9), it has been assumed that the orientation of the molecules is fixed. This allows one to separate the orientational dependence of the signal from the vibrational/librational dynamics. This is done by Taylor expanding the polarizability operator $\hat{\alpha}$ in terms of the vibrational/librational position operator q as $\hat{\alpha}_{ij} = \alpha_{ij}^o + \alpha_{ij}q + \cdots$. This allows separation into an orientation-dependent tensorial part and a part describing the vibrational/librational dynamics. The latter contains the anticommutator of the vibrational/librational position operator. It has been shown[29,38] that in a quantum Brownian-oscillator model it can be written as

$$\frac{i}{\hbar}\langle[q(\tau),q]_-\rangle_Q = \frac{1}{m\Omega}e^{-\gamma\pi/2}\sin(\Omega\tau), \tag{15}$$

where $\Omega = \sqrt{\omega^2 - \gamma^2/4}$, and m and ω are the mass and frequency of the Brownian oscillator. Of course, this crude model can be expanded by summing over a distribution of Brownian-oscillator modes with different masses and frequencies.

C. Magnetic-dipole and quadrupole interactions

First the RIKOA signal caused by interaction through a magnetic-dipole moment will be considered. In lowest order, there will be one interaction with the magnetic-dipole-moment operator while the remaining three interactions are with the electric-dipole-moment operator. The refractive signal is given by Eq. (7) and we will set $\mu_0\mathbf{H} \cong \mathbf{B}$ as the magnetization will be small. Using the expression for the *o*-ization Eq. (9), it can be seen that there are four terms: Three polarization terms with a magnetic-dipole interaction in the first, second, or third field interaction and a magnetization (see Fig. 2). It then follows that

$$S = -\frac{N\omega_0}{16}\frac{(E^{0,\text{pump}})^2(E^{0,\text{probe}})^2}{c}\,\text{Re}\int_0^\infty d\tau G(\tau) \times T^{\text{RIKOA1}}\frac{i}{\hbar}\langle[q(\tau),q]_-\rangle_Q, \tag{16}$$

where

$$T^{\mathrm{RIKOA1}} = i\begin{pmatrix} +\langle \alpha_{kl}\gamma_{ij}\rangle e_i b_j^* e_k e_l^* - \langle \alpha_{kl}\gamma_{ji}\rangle b_i e_j^* e_k e_l^* \\ +\langle \gamma_{kl}\alpha_{ij}\rangle e_i e_j^* e_k b_l^* - \langle \gamma_{lk}\alpha_{ij}\rangle e_i e_j^* b_k e_l^* \end{pmatrix} \tag{17}$$

and

$$\gamma_{ij} = \frac{d}{\hbar\Delta dq}\mu_i M_j \tag{18}$$

is the first derivative with respect to the vibrational coordinate of the electric-dipole–magnetic-dipole optical activity tensor[26] often denoted by the symbol G'. As before, in Eq. (16) the indices i and j refer to the pump-laser field, and k and l to the probe-laser field, it has been assumed that the laser is far off resonance, and that the orientation of the molecules is fixed.

The derivation of an expression for the RIKOA signal involving one interaction through the electric-quadrupole tensor follows along the same lines as that involving the magnetic-dipole moment. There are again four terms: three polarization terms in which the electric-quadrupole interaction comes in first, second, or third place, and one polarization term involving the expectation value of the electric quadrupole. The resulting expression for the signal is the same as Eq. (16) but with the tensorial part replaced by

$$T^{\mathrm{RIKOA2}} = i\frac{1}{3}\begin{bmatrix} +\langle \alpha_{kl}\theta_{ijm}\rangle e_i e_j^* e_k e_l^* \kappa_m^{\mathrm{pump}} \\ -\langle \alpha_{kl}\theta_{jim}\rangle e_i e_j^* e_k e_l^* \kappa_m^{\mathrm{pump}} \\ +\langle \theta_{klm}\alpha_{ij}\rangle e_i e_j^* e_k e_l^* \kappa_m^{\mathrm{probe}} \\ -\langle \theta_{lkm}\alpha_{ij}\rangle e_i e_j^* e_k e_l^* \kappa_m^{\mathrm{probe}} \end{bmatrix}, \tag{19}$$

where

$$\theta_{ijk} \equiv \omega_0 \frac{d}{\hbar\Delta dq}\mu_i Q_{jk} \tag{20}$$

is the first derivative with respect to the vibrational coordinate of the electric-dipole–electric-quadrupole tensor[26] often denoted by the symbol A. It can be seen that if both pump and probe lasers propagate in the same direction, T^{RIKOA2} has a form very similar to that of T^{RIKOA1}.

D. Tensors and tensor averages

The equations for the OHD-RIKES Eq. (11) and OHD-RIKOA Eq. (16) signal strengths involve orientational averages of tensor quantities [Eqs. (12), (17), and (19)]. The types of samples of interest for study with RIKES and RIKOA are isotropic (liquids, solutions, or glasses) and therefore the tensor quantities need to be averaged over an isotropic distribution. Simple methods exist to perform such averages[39] and the elements of the averaged tensor can then be found if the fields are defined. It is useful to define tensor invariants.[27]

$$\alpha^{(\mathrm{iso})} \equiv \frac{1}{3}\alpha_{ij}\delta_{ij}, \tag{21}$$

$$\gamma^{(\mathrm{iso})} \equiv \frac{1}{3}\gamma_{ij}\delta_{ij}. \tag{22}$$

The latter two are the isotropic invariants of the polarizability tensor and the electric-dipole–magnetic-dipole optical-activity tensor. It can easily be checked that the equivalent isotropic invariant of the electric-dipole–electric-quadrupole tensor ($\theta_{ijk}\varepsilon_{ijk}$ where ε_{ijk} is the Levi–Civita tensor) vanishes on account of the symmetry of the quadrupole tensor [Eq. (4)]. Furthermore,

$$\beta(\alpha) \equiv \frac{1}{2}(3\alpha_{ij}\alpha_{ij} - \alpha_{ii}\alpha_{jj}), \tag{23}$$

$$\beta(\gamma) \equiv \frac{1}{2}(3\alpha_{ij}\gamma_{ij} - \alpha_{ii}\gamma_{jj}), \tag{24}$$

and

$$\beta(\theta) \equiv \frac{1}{2}\alpha_{ij}\varepsilon_{ikl}\theta_{klj} \tag{25}$$

are the symmetric anisotropic invariants.

In order to compare RIKES with RIKOA, it will now be assumed that both the pump and probe beams propagate in the positive z direction. The electric-field polarization will be indicated by X or Y for linearly polarized light, and $R=2^{-1/2}(X-iY)$ and $L=2^{-1/2}(X+iY)$ for right and left circularly polarized light. The tensorial terms [Eqs. (12), (17), and (19)] depend on the polarization of the two pump fields and the two probe fields. The various terms will be denoted as T_{IJKL} where I and J refer to the pump-field polarization, K to the probe field polarization, and L to the detected polarization.

For OHD-RIKES the well-known result

$$\begin{aligned} T_{XXXX}^{\mathrm{RIKES}} &= T_{YYYY}^{\mathrm{RIKES}} = (\alpha^{(\mathrm{iso})})^2 + \frac{4}{45}\beta(\alpha), \\ T_{XXYY}^{\mathrm{RIKES}} &= (\alpha^{(\mathrm{iso})})^2 - \frac{2}{45}\beta(\alpha), \\ T_{XXXX}^{\mathrm{RIKES}} &- T_{XXYY}^{\mathrm{RIKES}} = \frac{6}{45}\beta(\alpha) \end{aligned} \tag{26}$$

is found after orientational averaging. Standard OHD-RIKES experiments measure[1,22,38] $T_{XXXX}^{\mathrm{RIKES}} - T_{XXYY}^{\mathrm{RIKES}}$ and therefore the signal only depends on the anisotropic invariant of the polarizability tensor. Experimentally, one effectively measures the difference in the refractive index for a probe field parallel to the pump field ($T_{XXXX}^{\mathrm{RIKES}}$) and one perpendicular to the pump field ($T_{XXYY}^{\mathrm{RIKES}}$). A variation on OHD-RIKES called spatially masked optical Kerr effect (SMOKE) directly measures $T_{XXXX}^{\mathrm{RIKES}}$ and $T_{XXYY}^{\mathrm{RIKES}}$ in order to determine the isotropic and anisotropic invariants separately.[22] It is also found that

$$\begin{aligned} T_{LLLL}^{\mathrm{RIKES}} &= T_{RRRR}^{\mathrm{RIKES}} = T_{RRLL}^{\mathrm{RIKES}} = T_{LLRR}^{\mathrm{RIKES}} = T_{XXRR}^{\mathrm{RIKES}} = T_{XXLL}^{\mathrm{RIKES}} \\ &= T_{LLXX}^{\mathrm{RIKES}} = T_{RRXX}^{\mathrm{RIKES}} = (\alpha^{(\mathrm{iso})})^2 + \frac{1}{45}\beta(\alpha), \end{aligned} \tag{27}$$

which means that if only electric-dipole-moment transitions

are considered, there is (unsurprisingly) no optical activity as there is no difference in the refractive index for left and right circularly polarized light.

Similarly, the orientational averages of the magnetic-dipole OHD-RIKOA signal can be performed for pump and probe beams traveling in the positive z direction. For convenience, we will define

$$N \equiv 2\alpha^{\mathrm{iso}}\gamma^{\mathrm{iso}} + \frac{2}{45}\beta(\gamma). \tag{28}$$

The important terms in OHD-RIKES vanish in OHD-RIKOA, i.e.,

$$T^{\mathrm{RIKOA1}}_{XXXX} = T^{\mathrm{RIKOA1}}_{XXYY} = 0. \tag{29}$$

It would seem logical that only those terms involving circularly polarized light have a value in RIKOA. For example, if the pump laser is right circularly polarized, it is found for the various signal components:

$$\begin{aligned} T^{\mathrm{RIKOA1}}_{RRXX} &= T^{\mathrm{RIKOA1}}_{RRYY} = N, \\ T^{\mathrm{RIKOA1}}_{RRYX} &= -T^{\mathrm{RIKOA1}}_{RRXY} = iN, \end{aligned} \tag{30}$$

and the exact same result is obtained when the pump-laser beam is left circularly polarized. For an x-polarized pump-laser field, one has besides Eq. (29) also

$$T^{\mathrm{RIKOA1}}_{XXYX} = -T^{\mathrm{RIKOA1}}_{XXXY} = iN \tag{31}$$

and an identical result for a y-polarized pump-laser field.

It is not immediately obvious what these results mean for a practical OHD-RIKOA experiment. In fact, it is not even immediately obvious that the above expressions represent an optical-activity signal. It can be calculated, however, that, for example,

$$T^{\mathrm{RIKOA1}}_{RRRR} - T^{\mathrm{RIKOA2}}_{RRLL} = 2N. \tag{32}$$

One obtains the exact same result for a left circularly polarized pump field and for an x- or y-polarized pump field. This shows the optical-activity effect: Independent of the pump-field polarization, a difference in refractive index is induced in the sample between that for a left or right circularly polarized probe field.

The orientational averages of the electric-quadrupole OHD-RIKOA signal for pump and probe beams traveling in the positive z direction give a similar result to that involving the magnetic-dipole moment. The various signal components have the same structure as those listed in Eq. (30) except N is replaced by M, defined by

$$M \equiv \frac{2}{45}\beta(\theta). \tag{33}$$

E. Practical description with Jones matrices

The signal components as listed above do not give a great deal of insight into the actual optical process taking place. It is useful to rewrite these results in matrix form by defining x-polarized light as the vector $(1,0)^T$ and y-polarized light as $(0,1)^T$ The optical interaction of the probe field with the (pump-pulse perturbed) sample can then be written in matrix form as

$$\mathbf{s} = \hat{T} \cdot \mathbf{p}, \tag{34}$$

where $\mathbf{p}$ is the electric-field vector of the probe-laser pulse, and $\mathbf{s}$ the detected polarization. In this notation, the OHD-RIKES signal due to an x-polarized pump [Eq. (26)] can be summarized as

$$\hat{T} = \begin{pmatrix} A & 0 \\ 0 & B \end{pmatrix}, \tag{35}$$

where

$$A = (\alpha^{(\mathrm{iso})})^2 + \frac{4}{45}\beta(\alpha), \quad B = (\alpha^{(\mathrm{iso})})^2 - \frac{2}{45}\beta(\alpha). \tag{36}$$

Since the signal as calculated here corresponds to a refractive-index change, the signal matrix can be related to the Jones matrix[36] $\hat{J}$ by

$$\hat{T} = i(\hat{J} - \hat{1}), \tag{37}$$

where $\hat{1}$ is the unit matrix. The reason for the unit matrix appearing is that in the derivation above, only the third-order polarization and magnetization have been considered and not the first-order contribution. Using the above expression, one can determine the Jones matrix for the OHD-RIKES signal induced by an x-polarized pump field as

$$\hat{J}^{\mathrm{RIKES}} = \begin{pmatrix} 1 - iA & 0 \\ 0 & 1 - iB \end{pmatrix}. \tag{38}$$

This is the Jones matrix of a retardation plate[36] aligned with the x axis. Due to our use of Eq. (7), this result is only valid in the small-signal limit or, equivalently, in the limit of vanishingly small retardation. It is, of course, a well-known result and shows, for example, that x-polarized light on propagating through the pumped sample will acquire a phase shift $\exp(-iA) \cong 1 - iA$.

The signal components for OHD-RIKOA involving the magnetic-dipole moment can be treated in the same way. The corresponding Jones matrices for a sample pumped by a right circularly, left circularly, or linearly polarized pump field are

$$\hat{J}^{\mathrm{RIKOA1},R\text{-pump}} = \begin{pmatrix} 1 - iN & N \\ -N & 1 - iN \end{pmatrix}, \tag{39}$$

$$\hat{J}^{\mathrm{RIKOA1},L\text{-pump}} = \begin{pmatrix} 1 + iN & N \\ -N & 1 + iN \end{pmatrix}, \tag{40}$$

and

$$\hat{J}^{\mathrm{RIKOA1},X \text{ or } Y\text{-pump}} = \begin{pmatrix} 1 & N \\ -N & 1 \end{pmatrix}. \tag{41}$$

The Jones matrices for OHD-RIKOA involving the electric-quadrupole moment are very similar but with N replaced by M. It is straightforward to check that the OHD-RIKOA Jones matrices are invariant under rotation in the x-y plane. Using the Jones matrices, it is now easy to see what types of signals will be generated. For example,

$$\hat{J}^{\mathrm{RIKOA1},R\text{-pump}}\mathbf{X} = \mathbf{X} - iN\sqrt{2}\mathbf{R},$$
$$\hat{J}^{\mathrm{RIKOA1},R\text{-pump}}\mathbf{Y} = \mathbf{Y} + N\sqrt{2}\mathbf{R}, \tag{42}$$

that is, when the sample is pumped by a right circularly polarized pump, a linearly polarized probe will acquire a small R-polarized component and similarly for an L-polarized pump. The OHD-RIKOA Jones matrix for a linearly polarized pump field [Eq. (41)] is a counterclockwise rotation (for $N>0$ and right-handed axes). Another way of looking at this is

$$\hat{J}^{\mathrm{RIKOA1},X \text{ or } Y\text{-pump}}\mathbf{L} = \mathbf{L}(1 + iN),$$
$$\hat{J}^{\mathrm{RIKOA1},X \text{ or } Y\text{-pump}}\mathbf{R} = \mathbf{R}(1 - iN), \tag{43}$$

that is, the pump pulse induces a retardation between right and left circularly polarized probe light. The sign and magnitude of the retardation is the same for all types of pump-field polarization. The Jones matrices for OHD-RIKOA involving the quadrupole moment are slightly different but they still produce the same retardation difference for all pump-field polarizations. The total circular retardation is then of magnitude $2N+2M$.

How would one measure this retardation difference? One method would be to use a probe-laser field polarized under 45°, followed by the sample, and measurement of the difference between X and Y polarized light intensities. This is similar to a balanced-detection scheme used previously in OHD-RIKES.[3,11,13,15] In Jones-matrix notation:

$$\mathbf{j} = \hat{J}^{\mathrm{RIKOA},R/L/X/Y\text{-pump}} \cdot \frac{1}{\sqrt{2}}\begin{pmatrix}1\\1\end{pmatrix}. \tag{44}$$

The balanced signal is then

$$j_X^2 - j_Y^2 = 2N + 2M, \tag{45}$$

which is linear in the circular retardation and independent of pump polarization. Thus, even though the Jones matrices for the different pump polarizations in Eqs. (39)–(41) are slightly different, the balanced signal in Eq. (45) is the same for all.

III. CONCLUSION AND SUMMARY

Taking into account one interaction with either a magnetic-dipole moment or electric-quadrupole moment in the standard OHD-RIKES technique leads to a new type of signal referred to as OHD-RIKOA. In OHD-RIKES, a linearly polarized pump pulse perturbs an isotropic sample and causes a different refractive index for light polarized parallel and perpendicular to the pump polarization. In OHD-RIKOA, a pump pulse of any polarization causes a difference in the refractive index for right versus left circularly polarized light. By choosing the appropriate polarization conditions in the experiment, this circular retardation can be measured directly in a balanced-detection setup. The full expression for the OHD-RIKOA signal is

$$S_{\mathrm{RIKOA}} = -\frac{N\omega_0}{16}\frac{(E_0^{\mathrm{pump}})^2(E_0^{\mathrm{probe}})^2}{c}\left[4\alpha^{\mathrm{iso}}\gamma^{\mathrm{iso}} + \frac{4}{45}\beta(\gamma) + \frac{4}{45}\beta(\theta)\right]\mathrm{Re}\int_0^\infty d\tau G(\tau)\frac{i}{\hbar}\langle[q(\tau),q]_-\rangle_Q, \tag{46}$$

which is very similar but not quite identical to the expression for depolarized Raman optical activity (ROA) scattering in the forward direction. However, because of Eq. (3), our definition of the electric-dipole–magnetic-dipole optical-activity tensor γ is of opposite sign to the standard definition of G'.[26,27] Therefore, the OHD-RIKOA signal does, in fact, contain the exact same information as depolarized ROA. This conclusion is similar to the earlier discovery[38] that the OHD-RIKES signal contains the same information as depolarized Raman scattering. The vibrational/librational response function for OHD-RIKES and OHD-RIKOA Eq. (15) differs from that of spontaneous Raman scattering (and ROA) resulting in the suppression of the Rayleigh peak in the time-resolved experiments. It is for this reason that OHD-RIKES and OHD-RIKOA are especially sensitive in the low-frequency region as compared to their normal Raman-scattering analogs. We have therefore shown that it should be possible to measure the low-frequency ROA spectrum using the chiroptical analog of OHD-RIKES.

That leaves one topic untouched: The magnitude and sign of the tensor invariants appearing in Eq. (46). It is well known that these tensor invariants can only have a value in chiral molecules. Therefore, it is clear that the first OHD-RIKOA experiments should be performed in pure liquids of chiral molecules. The technique would also have promising applications to the study of intermediate-frequency modes in peptides and proteins[11–13] where it may be able to clearly distinguish backbone torsional modes from hydrogen-bond stretching modes. It is impossible to predict at this point whether the various intermediate-frequency modes that are typically identified in a fit to an OHD-RIKES spectrum will have very different or similar tensor invariants. From previous SMOKE measurements[8,22] it is known that the isotropic invariant of the (electric-dipole) polarizability tensor is very small compared to the anisotropic invariant for the intermediate frequency modes in liquids. This suggests that the OHD-RIKOA signal will mostly depend on the magnitude and sign of $\beta(\gamma)$ and $\beta(\theta)$. In an idealized molecular model of axially symmetric bonds,[27] $\alpha^{\mathrm{iso}}\gamma^{\mathrm{iso}}=0$ and $\beta(\gamma)=-\beta(\theta)$, and the OHD-RIKOA signal would vanish in the forward direction (as would the ROA scattering amplitude). However, this model is certain to be too simplistic in most cases and there is sufficient evidence for the appearance of ROA bands of low-frequency modes in the forward direction in small chiral molecules.[26]

In setting up an OHD-RIKOA experiment, it will be very important to suppress any OHD-RIKES signals, which could be three orders of magnitude larger. In the scheme proposed here [linearly polarized probe pulse, see Eq. (44)], OHD-RIKES signals could be suppressed by either using a circularly polarized pump pulse or a linearly polarized pump pulse with the polarization either parallel or perpendicular to that of the probe pulse. The relative polarizations of the

pump and the probe pulses will have to be controlled with an accuracy better than 1:1000. Therefore, parallel or perpendicular polarization would appear to be experimentally advantageous as one could use a single good quality polarizer (or polarizing beamsplitter) to set the polarization of pump and probe fields at the same time. Samples with significant linear optical rotatory dispersion or dichroism would rotate the polarization of pump and probe fields equally and therefore it should be straightforward to cancel such effects by rotating either the input or the output polarizations in order to maintain balanced detection. If the pump and probe lasers approach an intermediate (electronic) resonance, this would enhance the strength of both RIKES and RIKOA signals. Resonance should be avoided, however, as dichroic signals (due to resonant pump-probe effects) would be mistaken for RIKOA signals. Signals due to SMOKE (Ref. 22) or multiphoton absorption should be canceled out in the balanced-detection scheme described here.

ACKNOWLEDGMENTS

Discussions with Laurence Barron and Lutz Hecht of Glasgow University on Raman Optical Activity and related optical-activity phenomena are gratefully acknowledged. Without them, this paper could not have been written. Discussions on the optical Kerr effect and other ultrafast polarization spectroscopies with Neil Hunt and David Turton are also gratefully acknowledged. This research has been supported by grants from EPSRC and the Leverhulme Trust.

[1] N. A. Smith and S. R. Meech, Int. Rev. Phys. Chem. **21**, 75 (2002).
[2] K. Wynne, C. Galli, and R. M. Hochstrasser, Chem. Phys. Lett. **193**, 17 (1992); Y. J. Chang and E. W. Castner, J. Chem. Phys. **99**, 7289 (1993); **99**, 113 (1993); E. W. Castner, Y. J. Chang, Y. C. Chu, and G. E. Walrafen, *ibid.* **102**, 653 (1995); S. Palese, S. Mukamel, R. J. D. Miller, and W. T. Lotshaw, J. Phys. Chem. **100**, 10380 (1996); N. A. Smith, S. Lin, S. R. Meech, and K. Yoshihara, *ibid.* **101**, 3641 (1997); K. Winkler, J. Lindner, and P. Vohringer, Phys. Chem. Chem. Phys. **4**, 2144 (2002).
[3] G. Giraud, C. Gordon, I. R. Dunkin, and K. Wynne, J. Chem. Phys. **199**, 464 (2003).
[4] G. Giraud and K. Wynne, J. Chem. Phys. **119**, 11753 (2003).
[5] Y. J. Chang and E. W. Castner, J. Phys. Chem. **100**, 3330 (1996); B. Ratajska-Gadomska, W. Gadomski, P. Wiewior, and C. Radzewicz, J. Chem. Phys. **108**, 8489 (1998); M. Ricci, P. Bartolini, R. Chelli, G. Cardini, S. Califano, and R. Righini, Phys. Chem. Chem. Phys. **3**, 2795 (2001).
[6] M. C. Beard, W. T. Lotshaw, T. M. Korter, E. J. Heilweil, and D. McMorrow, J. Phys. Chem. A **108**, 9348 (2004).
[7] H. Cang, J. Li, V. N. Novikov, and M. D. Fayer, J. Chem. Phys. **118**, 9303 (2003); B.-R. Hyun and E. L. Quitevis, Chem. Phys. Lett. **370**, 725 (2003).
[8] N. T. Hunt and S. R. Meech, J. Chem. Phys. **120**, 10828 (2004).
[9] N. P. Ernsting, G. M. Photiadis, H. Hennig, and T. Laurent, J. Phys. Chem. A **106**, 9159 (2002); P. P. Wiewior, H. Shirota, and E. W. Castner, J. Chem. Phys. **116**, 4643 (2002).
[10] A. Idrissi, P. Bartolini, M. Ricci, and R. Righini, J. Chem. Phys. **114**, 6774 (2001).
[11] G. Giraud and K. Wynne, J. Am. Chem. Soc. **124**, 12110 (2002).
[12] J. D. Eaves, C. J. Fecko, A. L. Stevens, P. Peng, and A. Tokmakoff, Chem. Phys. Lett. **376**, 20 (2003).
[13] G. Giraud, J. Karolin, and K. Wynne, Biophys. J. **85**, 1903 (2003).
[14] B. J. Loughnane, R. A. Farrer, A. Scodinu, T. Reilly, and J. T. Fourkas, J. Phys. Chem. B **104**, 5421 (2000); A. Scodinu and J. T. Fourkas, *ibid.* **106**, 10292 (2002); N. T. Hunt, A. A. Jaye, and S. R. Meech, *ibid.* **107**, 3405 (2003); N. T. Hunt, A. A. Jaye, A. Hellman, and S. R. Meech, *ibid.* **108**, 100 (2004).
[15] A. D. Slepkov, F. A. Hegmann, Y. Zhao, R. R. Tykwinski, and K. Kamada, J. Chem. Phys. **116**, 3834 (2002).
[16] D. McMorrow, N. Thantu, V. Kleiman, J. S. Melinger, and W. T. Lotshaw, J. Phys. Chem. A **105**, 7960 (2001).
[17] Y. Tanimura and S. Mukamel, J. Chem. Phys. **99**, 9496 (1993); V. Khidekel and S. Mukamel, Chem. Phys. Lett. **240**, 304 (1995); T. Steffen, J. T. Fourkas, and K. Duppen, J. Chem. Phys. **105**, 7364 (1996); V. Chernyak and S. Mukamel, *ibid.* **108**, 5812 (1998).
[18] A. Tokmakoff and G. R. Fleming, J. Chem. Phys. **106**, 2569 (1997); O. Golonzka, N. Demirdoven, M. Khalil, and A. Tokmakoff, *ibid.* **113**, 9893 (2000); L. J. Kaufman, D. A. Blank, and G. R. Fleming, *ibid.* **114**, 2312 (2001).
[19] K. J. Kubarych, C. J. Milne, S. Lin, V. Astinov, and R. J. D. Miller, J. Chem. Phys. **116**, 2016 (2002).
[20] J. C. Kirkwood and A. C. Albrecht, J. Raman Spectrosc. **31**, 107 (2000).
[21] S. Park, B. N. Flanders, X. Shang, R. A. Westervelt, J. Kim, and N. F. Scherer, J. Chem. Phys. **118**, 3917 (2003); D. F. Underwood and D. A. Blank, J. Phys. Chem. A **107**, 956 (2003).
[22] C. J. Fecko, J. D. Eaves, and A. Tokmakoff, J. Chem. Phys. **117**, 1139 (2002).
[23] P. W. Atkins and L. D. Barron, Mol. Phys. **16**, 453 (1969).
[24] L. D. Barron and A. D. Buckingham, Mol. Phys. **20**, 1111 (1971); L. Hecht and L. A. Nafie, *ibid.* **72**, 441 (1991).
[25] L. D. Barron, L. Hecht, E. W. Blanch, and A. F. Bell, Prog. Biophys. Mol. Biol. **73**, 1 (2000).
[26] L. D. Barron, L. Hecht, I. H. McColl, and E. W. Blanch, Mol. Phys. **102**, 731 (2004).
[27] L. D. Barron, *Molecular Light Scattering and Optical Activity*, 2nd ed. (Cambridge University Press, Cambridge, 2004).
[28] L. A. Nafie, R. K. Dukor, and T. B. Freedman, in *Handbook of Vibrational Spectroscopy*, edited by J. M. Chalmers and P. R. Griffiths (Wiley, Chichester, 2002).
[29] S. Mukamel, *Principles of Nonlinear Optical Spectroscopy* (Oxford University Press, New York, 1995).
[30] D. Heiman, R. W. Hellwarth, M. D. Levenson, and G. Martin, Phys. Rev. Lett. **36**, 189 (1976); J. J. Song and M. D. Levenson, J. Appl. Phys. **48**, 3496 (1977); G. Wagniere, J. Chem. Phys. **77**, 2786 (1982); J.-L. Oudar, C. Minot, and B. A. Garetz, *ibid.* **76**, 2227 (1982); M. Klein, M. Maier, and W. Prettl, Phys. Rev. B **28**, 6008 (1983); F. W. Schneider, R. Brakel, and H. Spiegel, Ber. Bunsenges. Phys. Chem. **93**, 304 (1989).
[31] W. J. Meath and E. A. Power, J. Phys. B **20**, 1945 (1987); H. Mesnil and F. Hache, Phys. Rev. Lett. **85**, 4257 (2000); M. Cho, J. Chem. Phys. **116**, 1562 (2002); M. Alexandre, G. Lemercier, C. Andraud, H. Mesnil, M. C. Schanne-Klein, and F. Hache, Synth. Met. **127**, 135 (2002); P. Fischer, A. D. Buckingham, K. Beckwitt, D. S. Wiersma, and F. W. Wise, Phys. Rev. Lett. **91**, 173901 (2003); S. Cheon and M. Cho, Phys. Rev. A **71**, 013808 (2005).
[32] M. Cho, J. Chem. Phys. **119**, 7003 (2003).
[33] D. L. Andrews, J. Chem. Phys. **72**, 4141 (1980).
[34] R. Loudon, *The Quantum Theory of Light*, 2nd ed. (Clarendon, Oxford, 1983).
[35] Y. R. Shen, *The Principles of Nonlinear Optics* (Wiley, New York, 1986).
[36] A. Yariv, *Optical Electronics*, 4th ed. (Harcourt, Fort Worth, 1991).
[37] T. Wagersreiter and S. Mukamel, J. Chem. Phys. **105**, 7995 (1996); W. Liang, S. Yokojima, and G. Chen, Chem. Phys. **289**, 175 (2003).
[38] M. Cho, M. Du, N. F. Scherer, G. R. Fleming, and S. Mukamel, J. Chem. Phys. **99**, 2410 (1993).
[39] D. P. Craig and T. Thirunamachandran, *Molecular Quantum Electrodynamics* (Academic, London, 1984).